Optimal structure for Resonant THz Detection of Plasmons-Polaritons in the 2D quantum wells

L. Cao, A.-S. Grimault-Jacquin*, and F. Aniel

[1]Institut d'Electronique Fondamentale, CNRS UMR 8622 Université Paris Sud 91405 Orsay cedex, France
*corresponding author: anne-sophie.grimault@u-psud.fr

Abstract

We investigate terahertz plasmon-polariton (PP) resonances for hetero-structures (AlGaN/GaN, SiGe/Si/SiGe, AlGaAs/GaAs and InAlN/GaN) with grating coupler in order to find the overall optimal structure showing the strongest absorption for terahertz detection (THz). We show by a parametric study (influence of geometric dimensions, electron concentration, temperature…) that refined and intense resonances can be obtained at specific frequency. GaN based heterostructures present the higher PP resonances at room temperature. The roles of the finite thicknesses of lossy metal grating and two dimensional gas (2DEG) layer on observed absorption are also investigated. Absorption spectra for three kinds of heterogeneous charge density profiles (piecewise, linear and parabolic) of 2DEG was investigated and compared for an AlGaAs/GaAs structure because some physical parameters such as the Fermi Level pinning at the interface semiconductor/air are well established only for this heterostructure. We show that the PP resonance (amplitude and frequency position) is modulated by the charge concentration but also by the metallisation biasing.

1. Introduction

Two dimensional electron gas (2DEG) presents a growing interest in the Terahertz (THz) frequency range for the development of compact, tunable, room temperature operating and low cost detectors and sources [1]. The high electron concentration, large electron mobility and mainly the complex dispersion relation of plasmons are the principle advantages of 2DEG confined in a quantum well (QW) based on heterostructures. From the aspect of device optimization, it is critical to study the properties of plasmon-polariton (PP), or the coupling between the two dimensional (2D) plasmon and the electromagnetic (EM) field. PP can be excited through metal grating deposited on top of heterostructures. Electron concentration below the metal fingers in the QW varies from that between metals because of the different barrier height in the two regions. As a bias voltage is applied on metals, the electron density can be controlled to achieve the tunability of PP resonances, forming the modulated 2DEG.

Band diagrams and electron transport properties of Si, Ge, SiGe, GaAs and GaN quantum well have been extensively studied in our group [2-5]. Simulations of PP in this article are based on the known material parameters. Among the typical heterostructures, AlGaAs/GaAs has smaller lattice mismatch, while the modulation doping is essential to achieve high electron density. SiGe/Si material in the IV-IV group, compatible with silicon technology, owns its main advantages over the III-V group materials: silicon is cheap, ans it can be used in mature and high manufacturing technology for integrated circuits [6]. High electron concentration and mobility have been obtained experimentally in modulation doped SiGe/Si heterostructures [7]. Recently, GaN based structures attract more attention in grating gated field effect transistors (FET) [8-10] due to the large electron density induced by polarizations without doping.

Many numerical and analytical methods have been developed to study such corrugated heterostructure. Allen et al. [11] initially solved the problem of grating coupled transmission of light through 2D plasmon in silicon metal-oxide-semiconductor FET (MOSFET) by an analytical perturbative method. Zheng et al. [12] generalized and improved the theory in regimes of high electron scattering time by a numerical non perturbative approach. Concerning complicated stratified system with perfect grating of finite thickness, Ager and Hughes [13] described a computational scattering matrix technique. This method was applied to study 2D plasmon in AlGaAs/GaAs system [14-15]. By considering the radiation capabilities of 2D plasmon through grating, Matov et al. [16] have calculated numerically the complex plasmon frequency in a heterostructure, where the grating was treated as planar perfect strips. In a later paper, Popov et al. [17] extended the EM theory with finite conductivity metal for THz emission and amplification in FET arrays. Muravjov et al. [8] demonstrated this last approach for THz detection in a AlGaN/GaN HEMT. However, all of these works ignored the thickness of the QW and the ohmic loss in the grating of finite thickness. Wendler et al. [18-19] analyzed the spectrum of quasi 2D plasmon in AlGaAs/GaAs with lossy 3D grating by means of the transfer matrix method. The periodic grating issue was solved by the equivalent coupled wave method (CWM) and modal expansion method (MEM). For the purpose of resonance tunability, Matov et al. [20] observed a dipole like resonant peak in a strongly modulated 2DEG system with semi-transparent NiCr grating.

Until now, direct comparisons of dispersion and absorption properties of quasi 2D plasmon in different structures coupled by the three dimensional (3D) lossy grating under

the same numerical method have not yet been reported.

In this work, we compares and synthesizes the coupling effect between incident EM wave and 2D plasmons in four typical heterostructures (AlGaN/GaN, SiGe/Si/SiGe, AlGaAs/GaAs and InAlN/GaN) based on reported real structure parameters in order to find out the best material for technical realization for THz detection. We used CWM for homogeneous and inhomogeneous 2DEG systems. For this latter case, the CWM was slightly modified. We demonstrate for the first time, that the commercial code ANSOFT HFSS [21] based on finite element method (FEM) can solve the sophisticated problem of periodic gated heterostructures. Section 2 focuses on the optimization of THz absorption in homogeneous 2DEG system through a parametric study (grating period, metal width, electron density, barrier thickness and temperature) in the frequency domain [0-5] THz. The roles of the finite thicknesses of lossy metal grating and 2DEG layer on observed absorption are also considered. Our quantitative results by both methods are in good agreement with the ones of previous papers [14,15, 22] using scattering matrix and Galerkin's methods, and other commercial software like Sentaurus [10].

Section 3 mainly concentrates on the tunability of PP resonances as a function of the polarizability in a modulated 2DEG system (inhomogeneous) by using the slightly modified CWM code. Section 4 gives the general conclusions and perspectives of this work.

2. Homogeneous 2DEG

2.1. Modeling of homogeneous 2DEG

The modeling of the 2DEG can be addressed through an anisotropic permittivity of the QW layer [19] or through a sheet Drude conductivity as in [8]. Both approaches were compared and provide the same results only if the 2DEG thickness is well below the plasmon wavelength. In order to couple the normally incident EM wave, periodic metallic grating is deposited at a distance of *d* from the 2DEG layer, as shown in Fig.1 for a typical heterostructure AlGaAs/GaAs. The substrate GaAs is assumed to be semi-infinite. Electric field is polarized along the x axis (TM wave), and the whole structure is assumed to be infinite in the plane x-y. Grating parameters are: period (L), metal width (W), thickness (t) and DC conductivity (σ_{GOLD}). The influences of *t* on the transmission spectrum become important when *t* is comparable to L [23].With the grating, the in-plane wave vector is modulated at $k_{xn} = 2\pi n/L$, where n is the order of scattered wave.

Electrons in the QW can move freely in x-y plane while their wavevector is quantified along the growth axis z. Its anisotropic permittivity component ε_{xx} (ε_{yy}) is modeled through the 3D Drude conductivity σ_{3D}, while ε_{zz} is kept as the static permittivity of the background material where 2DEG lies:

$$\varepsilon_{xx}(x\,|\,\omega) = \varepsilon_{yy}(x\,|\,\omega) = \varepsilon_s + \frac{j\sigma_{3D}(x\,|\,\omega)}{\omega\varepsilon_0}, \varepsilon_{zz} = \varepsilon_s \qquad (1)$$

and 3D conductivity:

$$\sigma_{3D}(x\,|\,\omega) = \frac{N_s(x)e^2\tau}{m^* d_{2DEG}(1 - j\omega\tau)} \qquad (2)$$

where ε_s is the relative permittivity of QW layer, ε_0 is the permittivity of vacuum, $N_s(x)$ is the sheet electron density in function of the position x in 2DEG layer, d_{2DEG} is the default width of QW, $\tau=\mu_{2DEG}m^*/e$ is the phenomenological electron scattering time, μ_{2DEG}, m* and e are the mobility, effective mass and unit charge of an electron, respectively. Both the barrier (ε_b) and substrate (ε_s) layers are supposed to be lossless by letting the imaginary part of the permittivity null.

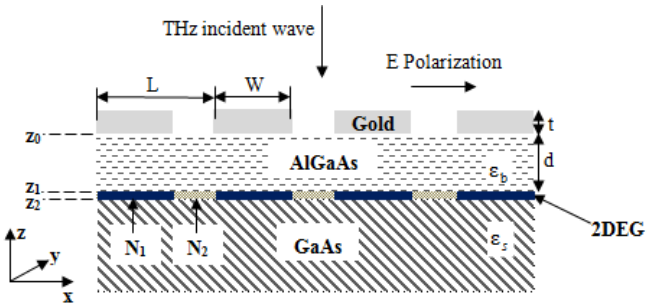

Fig. 1 Calculation model for AlGaAs/GaAs nominal structure

In this part we model the homogeneous 2DEG. Thus Ns(x) = Ns = N_1= N_2, where N_1 and N_2 are the electron densities below and between metal fingers, respectively. So the dielectric function is constant with position x at a frequency ω ($\varepsilon_{xx}(x|\omega)= \varepsilon_{xx}(\omega)$) according to (1) and (2).

Tab. 1 Parameters of the four nominal structures (W/L = 0.75)

Material	m^*/m_0	Ns (m^{-2})	L (μm)	d (nm)	μ_{2DEG} @300K (m^2/Vs)	μ_{2DEG} @77K (m^2/Vs)
AlGaN/GaN	0.22	1.2×10^{17}	2.2	25	0.2	1.0
InAlN/GaN	0.22	1.2×10^{17}	1.55	10	0.11	0.33
SiGe/Si/SiGe	0.19	5×10^{16}	1.3	25	0.3	3.2
AlGaAs/GaAs	0.063	10^{16}	1.0	25	0.8	5

Besides AlGaAs/GaAs, other three heterostructures will be studied for resonant THz detection at room and cryogenic temperatures namely SiGe/Si/SiGe, AlGaAs/GaAs and InAlN/GaN. The parameters of the standard structures including a 12 nm thick 2DEG layer are reported in Tab.1. Most of the material parameters of Tab.1 refer to existing publications [2-7, 24-28]. For the structure SiGe/Si/SiGe, the 12 nm thick QW layer (Si) is located between the barrier layer SiGe and the semi-infinite substrate SiGe. To facilitate comparisons, the first resonance is fixed at 1 THz via the grating period for epilayer stack chosen. L increases with electron density N_S when the barrier thickness *d* is fixed.

Two numerical methods are available for the calculation of spectrum (Transmission, Reflection and Absorption) in the multilayered structure with periodic metal grating:

- Commercial code ANSOFT HFSS based on FEM
- Indigenous program based on CWM [18]

In HFSS modeling, one period of 3D strained structure (unit cell) combined with periodic boundary conditions is modeled to simulate the infinite extension in x-y plane. The

spectra are calculated by the scattering parameters. The transmitted (T) and reflected (R) signals are normalized by the intensity of incident wave, and accordingly, absorption spectrum is obtained by A = 1-T-R. The roles played by the grating, dielectrics and 2DEG must be carefully separated to extract the intrinsic contribution of PP absorption on the absorption spectrum. Comparisons of the two approaches (CWM and FEM) on homogeneous 2DEG will be given.

Before turning to parametric sweep, we emphasize the influences of t, σ_{GOLD} and d_{2DEG} on the absorption spectra. Fig.2 shows the absorptions of nominal AlGaN/GaN structure calculated by CWM at different values of metal and 2DEG thicknesses. Fig.2 (a) plots only the conduction losses without 2DEG (N_s=0). As metal thickness t increases from 0.2 to 1 µm, the absorption grows accordingly due to larger ohmic losses in the metal. If t is comparable to L, the contribution of the conductor attenuation to the total absorption is no longer negligible, particularly at high frequency. In this condition, 3D grating with finite conductivity should be used in the modeling.

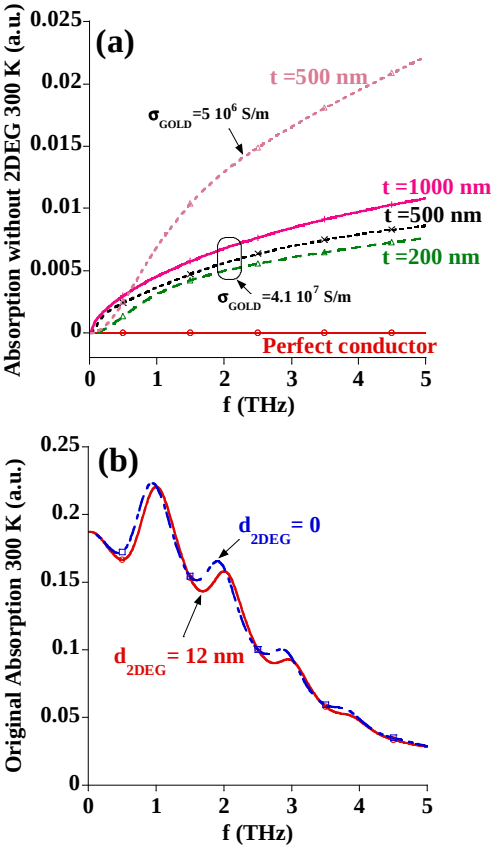

Fig. 2 Absorptions of nominal AlGaN/GaN structure calculated by CWM at 300 K, where L=2.2µm, W/L=0.75 and $N_s=1.2\times10^{17}$ m^{-2}. **(a)** Conduction losses in grating ($\sigma_{GOLD}=4.1\times10^7$ and 5×10^6 S/m) at different t. No 2DEG exists. Perfect grating is plotted for reference. **(b)** Original absorptions at different d_{2DEG}. Grating parameters: t=200 nm, $\sigma_{GOLD}=4.1\times10^7$ S/m

Of course, small metal conductivity (5×10^6 S/m) causes the increase of conduction losses at high frequency which may become a dominant factor in absorption. Fig.2 (b) shows the original absorptions (including contributions of grating and 2DEG) for exact 2D plasmon (d_{2DEG}=0, $\sigma_{2D}(\omega)=N_se^2\tau/(m^*(1-j\omega\tau))$ as in [8]) and quasi-2D plasmon (d_{2DEG}=12 nm) in our simulation. The absorption amplitude is nearly not affected by the thin 2DEG layer, however, the resonant positions for quasi-2D plasmon move to higher frequencies in particularly for higher orders of the scattered wave (n>1). Consequently, in the following simulations, the gold thickness and the gold conductivity are fixed to t=200 nm and $\sigma_{GOLD}=4.1\times10^7$ S/m respectively.

2.2. Optimal absorption spectrum for homogenous 2DEG

In this part, we try to find the optimal structure which has the maximum PP absorption among the four nominal materials at different temperatures by a parametric study (Ns, d, W/L and L) on PP resonances conducted by FEM, where the electron concentration is uniform as in Tab.1.

To reach strong PP excitation at a certain temperature, we should have high Ns, large W/L (0.25 to 0.9 in the modeling), and relatively small d_{2DEG}. A large d_{2DEG} leads to a fast decrease of the evanescent wave intensities at the vicinity of the grating. However, an extremely small d_{2DEG} reduces the coupling efficiency due to the strong screening effect of metals. PP resonant frequency increases monotonically with the growth of Ns and d_{2DEG}, but it decreases with the reduction of W when L is fixed. Similar results were reported for AlGaAs/GaAs ignoring finite QW width [14-15, 22]. Fig.3 (a) and (b) present the PP absorptions at 300 K and 77 K. The first peak is at f_1 = 1 THz while the other resonances can shift slightly from 2, 3 or 4 THz. The resonances become intense and narrow due to the improvement of the low field electron mobility μ_{2DEG} at 77 K and also due to the increased quality factor $\omega\tau$.

The PP dispersion frequency is proportional to the square root of the in-plane wave vector k_{xn} for 2D plasmon without surface metallization [29], and is proportional to k_{xn} for 2D plasmon overlaid by continuous metals [30]. Fig.4 shows the first resonant frequency f_1 versus the grating period L, where the relation $f_1 \propto k_{x1} \propto 1/L$ holds [8, 31] because W/L approaches 1 and the long wavelength approximation $k_{x1}d \ll 1$ is valid. The resonant frequencies of high scattered wave orders (n = 2, 3 and 4) in Fig.3 shift compared to the predicted totally screened 2D plasmon frequencies (2, 3 and 4 THz). This is linked to the fact that $k_{xn}d \ll 1$ is no longer valid and W/L does not equal to 1 (plasmon is partially screened by grating). Fig.4 clearly demonstrates that the frequency can be tuned between 0.5 and 3 THz through the grating period ranging from 0.5 to 5 µm.

Obviously, at 300 K, InAlN/GaN and AlGaN/GaN present the optimal PP resonances both in amplitude and in full width at half maximum (FWHM) at 1 THz. However, the structures AlGaAs/GaAs and SiGe/Si/SiGe also show equivalent resonant amplitudes at 77 K as those of GaN based materials (Tab.1).

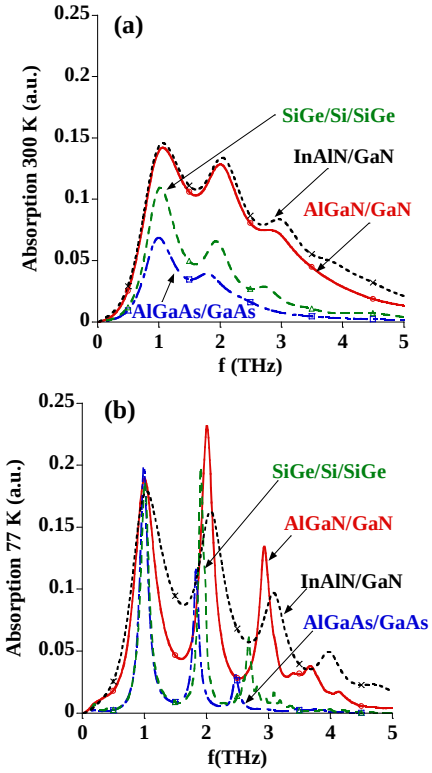

Fig. 3 Absorption spectra for the four nominal materials at (a) 300 K and (b) 77 K with W/L=0.75.

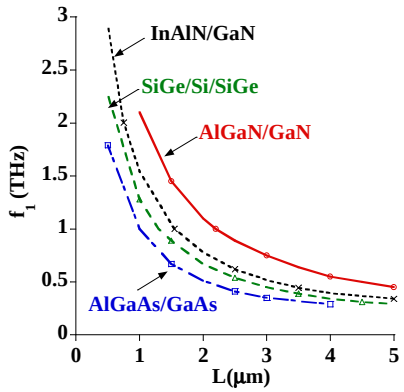

Fig. 4 Tunability of grating period on the first resonant peak position for the four nominal materials at 300 K. The ratio W/L is 0.75

Until now, we have considered the THz absorption in the homogeneous 2DEG system. After the sample is fabricated, a bias voltage could also be applied on the metallization to tune the PP resonances. At this condition, the electron distribution becomes inhomogeneous in x direction and this is what we will discuss in the next section.

3. Inhomogeneous 2DEG

A modulated 2DEG has been investigated without [32] and with [20, 33-34] grating on AlGaAs/GaAs. In most publications dealing with the PP absorption with grating coupler at zero bias, the electron distribution is assumed to be constant in x direction.

However, the electron density N_S varies within one period because the barrier height below the metallization and the Fermi levels pinning at the interface air/semiconductor leads to differences in N_S in the QW, as illustrated in Fig.1. In the case of highly modulated 2DEG, a distinct absorption peak can be observed, and its position can not be correctly predicted by a dipole like formula without the screening of metal [20, 35]. The screening effect of gold grating contributes to the decrease of resonant frequency. In theoretical modeling, the electron density distribution can be assumed piecewise constant or sinusoidal [33].

For the two heterostructures based on group III-nitride materials owing large bandgaps, a minor difference between barrier height and Fermi levels pinning does not alter greatly the electron density in the two regions (N_1 and N_2 in Fig.1), so the approximation of the homogeneous 2DEG is reasonable. Concerning the surface Fermi level at SiGe/oxide interface, as far as we know, no experimental data are available. Consequently, only AlGaAs/GaAs and AlGaN/GaN will be considered in the modeling of inhomogeneous 2DEG.

3.1. Modeling of inhomogeneous 2DEG

The electron density in 2DEG layer with and without metals on top of the structure can be calculated numerically by a self consistent one dimensional (1D) Poisson-Schrödinger solver in the frame of envelope function approximation and effective mass approximation [36]. In the simulation, for example for AlGaAs, in a 2 nm thick $Al_{0.3}Ga_{0.7}As$, separated by a 3 nm non intentionally doped (NID) $Al_{0.3}Ga_{0.7}As$ layer from the NID GaAs surface the doping level is $N_D = 2\times10^{19}$ cm^{-3}. The total thickness of AlGaAs is 25 nm as in section 2. The Au/Ti barrier height on the AlGaAs layer is 0.85 eV [37] while the surface potential is chosen to be 0.65 eV in the region of free semiconductor surface.

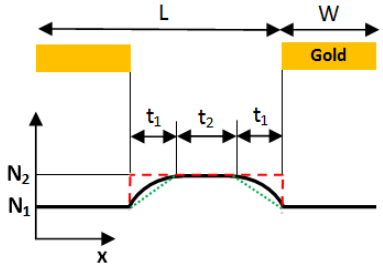

Fig. 5 Parabolic (solid), linear (dotted) and piecewise (broken) one dimensional distribution profiles of electron concentration in 2DEG layer

In modulated AlGaAs/GaAs structure, three kinds of 2DEG concentration profiles (piecewise, linear and parabolic) have been used to calculate the absorption spectrum (Fig.5), with CWM [18, 38] slightly modified to treat the issue of periodic 2DEG permittivity in QW layer. The 2DEG permittivity ε_{xx} will become position-dependent within a period L, while ε_{zz} is still a constant with x. The Fourier transform pair ε_{xx} and ε_n in the QW layer are then expressed as:

$$\varepsilon_{xx}(x\,|\,\omega)=\sum_{n=-\infty}^{+\infty}\varepsilon_n(\omega)\exp(j\frac{2\pi n}{L}x)$$
$$\varepsilon_n(\omega)=\frac{1}{L}\int_0^L\varepsilon_{xx}(x\,|\,\omega)\exp(-j\frac{2\pi n}{L}x)dx \quad (3)$$

The z-components of the wavevector in the 2DEG layer are found numerically as in the grating layer. Then the spectrum can be obtained from the same procedures discussed in the homogeneous 2DEG. For piecewise function, the electron densities below and between grating are constant and are assigned as N_1 and N_2 respectively. Explicit ε_n can be calculated through (3), while for linear and parabolic functions, the integration in (3) should be solved numerically to find ε_n. It should be noted that the present modeling approach remains local and further investigations require a non local 2DEG model based on Green functions.

Absorption spectra were calculated for all the three charge distribution profiles. The spatial extension of the transition zone has been calculated: t_1=20 nm (Fig.5), connecting the two adjacent regions with constant 2DEG concentrations. Calculations show that the three models present the same spectrum, because t_1 is much smaller than the gap width W_G = L - W (250 nm in minimum). Hence, the piecewise model has enough accuracy and it was also chosen for spectrum calculations in the structure AlGaAs/GaAs.

3.2. Absorption spectra for inhomogeneous 2DEG without bias voltage

The absorption spectra were calculated by FEM and CWM for AlGaN/GaN and AlGaAs/GaAs. Only the results of the nominal structure are presented in Fig.6. The electron density N_2 is varied around N_1 (1.2×10^{17} m^{-2}). The two methods provide results which are in good agreement for the two heterostructures.

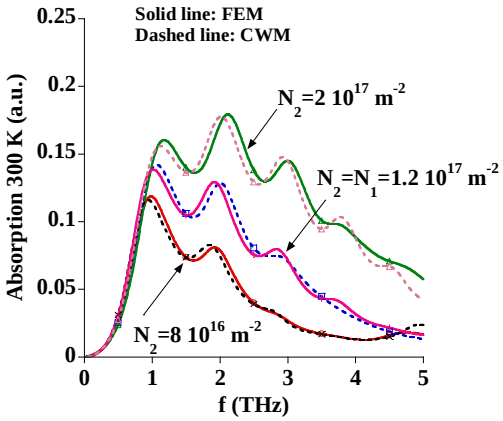

Fig. 6 Comparisons of the two numerical methods: Absorptions of nominal AlGaN/GaN structure with different N_2 at 300 K, W/L=0.75 and $N_1=1.2\times10^{17}$ m^{-2} (solid: FEM, dashed: CWM).

Larger N_2 yields stronger PP resonant frequency, larger absorption, and more observed resonances. This tendency is qualitatively consistent with the one obtained in homogeneous 2DEG.

3.3. Absorption spectra for voltage modulated inhomogeneous 2DEG

In this section, we present numerical results on modulated AlGaAs/GaAs system using solely CWM. Now, we turn to the influence of "gate" biasing on the absorption spectrum. N_2 is kept constant while N_1 is modulated between 0.12×10^{16} m^{-2} and 1.65×10^{16} m^{-2}. The influence of N_1 on the absorption spectrum of the AlGaAs/GaAs structure is shown in Fig.7 at W/L=0.75.

When applying a biasing voltage V_G on the grating, N_1 (see Fig.1) below metal fingers will be modified. At V_G=0.2 V, homogeneous 2DEG (N_1=N_2) is formed and the voltages around 0.2 V will change slightly N_1. Large negative V_G can greatly reduce N_1. Details on V_G induced variation of N_1 are in the index of Fig.7. Thus, the tunability of PP resonance frequency in the absorption spectrum can be realized by varying V_G.Two main observations can be made:

(1) In comparison with the homogeneous 2DEG (N_1 = N_2), a slightly large (small) N_1 will shift the resonance to high (low) frequency. This is because the screened plasmon frequency increases monotonically with electron density. The piecewise constant 2DEG is not equivalent to a homogeneous 2DEG with an average concentration N_{avg} = $N_1W/L + N_2W_G/L$. Indeed, the screened and unscreened plasmons follow different dispersions [39] and absorption mechanisms [34].

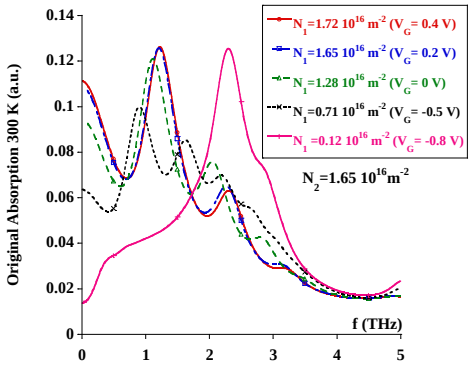

Fig. 7 Absorption spectrum of the AlGaAs/GaAs structure with modulated N_1 at 300 K. The piecewise constant model is used with $N_2=1.65\times10^{16}$ m^{-2} , L=1μm and W=0.75μm

(2) The absorption is reduced by decreasing N_1. At $N_1=0.12\times10^{16}$ m^{-2} (N_1 << N_2), the amplitude (at 0.4 THz) becomes not discernible due to the extremely small N_1. And a new resonance with substantial amplitude occurs and dominates at a higher frequency (2.3 THz). This suggests that the unscreened plasmon in the region W_G (=L-W) plays a most important role in the absorption. The references [20] and [35] showed there is a dipole like mode in the regime of strong modulation. Using the wavevector k = π/W_G, the calculated dipole oscillation frequency is 3.08 THz, which differs from the observed 2.3 THz. This difference should be due to an unscreened effect which can be obtained experimentally with a semitransparent NiCr grating [20]. Hence, it is equivalent to the case of modulated 2DEG without grating (open surface) as in [40]. Indeed, the

simulated dominant peak without grating is located at 3.18 THz (not shown here). This value is close to the one calculated at 3.08 THz if an error less than 5% is authorized [20]. We conclude that the metal grating with high conductivity can also strongly screen the plasmon in the open surface region, even if the electron density below metals is nearly zero. The dominant peak shifts to a low frequency due to this screening. Moreover, it is noticed that the dominant peak at 2.3 THz is not equivalent to the unscreened plasmon frequency (3.87 THz with $k = \pi/W_G$) as discussed in [34].

4. Conclusions

In conclusion, the effectiveness of the coupling between normally incident THz wave and quasi 2D plasmon in four heterostructures (AlGaN/GaN, InAlN/GaN, SiGe/Si/SiGe, and AlGaAs/GaAs) has been calculated using HFSS software and indigenous CWM model. The two approaches agree very well. The overall optimal heterostructure which has the maximum absorption due to the excitation of plasmon polariton has been proven to be the nitride based materials. A large electron concentration could be formed due to the high spontaneous and piezoelectric polarizations without any doping. Other structures also show interesting performances at cryogenic temperature because of the dramatic increase of electron momentum relaxation time.

The situation of an inhomogeneous 2DEG in the QW has also been investigated. Without biasing, three non uniform 2DEG profile models (piecewise, linear and parabolic) have been compared by CWM for the structure AlGaAs/GaAs. They are equivalent because the calculated small width t_1 of the transition region is small in comparison with the gap width W_G. For the inhomogeneous electron distribution in AlGaAs/GaAs, the resonant shifts to the lowest frequency because N_1 is inferior than N_2. For nitride based materials, the effect of inhomogeneous 2DEG is not obvious. Finally, when a bias is applied on metals, the excitation of the unscreened plasmon shows considerable absorption in the regime of strong modulation ($N_1 < N_2$), following a manner different from the grating screened plasmon. Further investigations are still needed. As the geometrical parameters and nature material, the bias voltage also plays a key role in the PP resonance tenability. The perspectives of this work are to take into account the non locality of the dielectric permittivity in the QW and also to investigate the response of a finite number of metal strips to the incident THz pulse.

References

1. W.Knap et al., J. Infrared Milli Terahz Waves, 30, 1319-1337 (2009).
2. F.Aniel et al., Journal de physique IV, 6, 145-149 (1996).
3. F.Aniel et al., IEEE Trans. Elec. Dev., 47, 1477-1483 (2000).
4. Soline Richard, Frédéric Aniel, and Guy Fishman, Physical Review B, 70, 235204 (2004).
5. Soline Richard et al., Proceeding of ESSDERC, France, 363-366(2005).
6. Douglas J Paul, Semiconductor Science and Technology, 19, R75-R108 (2004).
7. K.Ismail et al., Appl. Phys. Lett., 66, 1077-1079 (1995).
8. Muravjov et al., Appl. Phys. Lett. , 96, 042105 (2010).
9. Viacheslav V.Popov, J Infrared Milli Terahz Waves, 32, 1178-1191 (2011).
10. Lin Wang et al., Appl. Phys. Lett. , 100, 123501, 2012.
11. S.J.Allen, Jr.,D.C.Tsui and R.A.Logan., Phys. Rev. Lett. , 38, 980-982 (1977).
12. Lian Zheng, W.L.Schaich, and A.H.MacDonald, 41, 8493-8499 (1990).
13. C.D.Ager, and H.P.Hughes, Physical Review B, 44, 13452-13465 (1991).
14. R.E.Tyson, D.E.Bangert, and H.P.Hughes, J.Appl.Phys., 76, 5509-5515 (1994).
15. C.D.Ager, R.J.Wilkinson, and H.P.Hughes, J.Appl.Phys., 71, 1322-1326 (1992).
16. O.R.Matov, O.V.Polischuk, and V.V.Popov, Int. J. Infrared Milli Waves, 14, 1455-1470 (1993).
17. V.V.Popov, G.M.Tsymbalov and M.S.Shur, J. Phys.: Condens. Matter, 20, 384208 (2008).
18. L.Wendler, N.Finger and E.Gornik, Infrared Physics & Technology, 46, 291-307 (2005).
19. L. Wendler, T. Kraft, Physica B, 271, 33-98 (1999).
20. O.R.Matov, O.V.Polischuk, and V.V.Popov, J. Exp. Theor. Phys., 95, 505-510 (2002).
21. http://www.ansys.com/
22. S.A.Mikhailov, Physical Review B, 58, 1517-1532 (1998).
23. Lian Zheng, and W.L.Schaich, Phys. Rev. B, 43, 4515-4518 (1991).
24. M.A.di Forte-Poisson et al., Phys.Stat.Sol.(a), 203, 185-193 (2006).
25. M.-A.di Forte Poisson et al., Phys.Stat.Sol.(c), 7, 1317-1324 (2010).
26. Hidemi Takakuwa et al., IEEE Trans. Elec. Dev., ED-33, 595-600 (1986).
27. R.Fischer et al., Electronics Letters, 20, 945-947 (1984).
28. S.F.Nelson et al., Appl.Phys.Lett., 63, 367-369 (1993).
29. Noriyuki Okisu et al., Appl. Phys. Lett. , 48, No.12 (1986).
30. Adolfo Eguiluz, et al., Phys. Rev. B, 11, 4989-4993 (1975).
31. K.Hirakawa et al., Appl. Phys. Lett., 67, 2326-2328 (1995).
32. O.R.Matov, O.F.Meshkov, and V.V.Popov, J. of Experimental and Theoretical Physics, 86, 538-544 (1988).
33. C.D.Ager, and H.P.Hughes, Sol. State Communications, 83, 627-633 (1992)
34. D.V.Fateev, V.V.Popov, and M.S.Shur, Semiconductors, 44, 1406-1413(2010).
35. V.V.Popov et al, J. Appl. Phys., 94, 3556-3562 (2003).
36. G.L.Snider, I.-H.Tan, and E.L.Hu, J. Appl. Phys., 68, 2849-2853 (1990).
37. D.H.Zhang, Mat. Sci. Eng., B60, 189-193 (1999).
38. Lifeng Li, J.Opt.Soc.Am.A, 13, 1870-1876 (1996).
39. M. Nakayama, J. Phys. Soc. Jpn., 36, 393-398 (1974).
40. U.Mackens et al. Phys. Rev. Lett., 53, 1485-1488 (1984).